applied sciences

MDPI

Article

Towards Mode-Multiplexed Fiber Sensors: An Investigation on the Spectral Response of Etched Graded Index OM4 Multi-Mode Fiber with Bragg grating for Refractive Index and Temperature Measurement

Kort Bremer [1,*], Lourdes Shanika Malindi Alwis [2], Yulong Zheng [1] and Bernhard Wilhelm Roth [1,3]

1 Hannover Centre for Optical Technologies (HOT), Leibniz University Hannover, 30167 Hannover, Germany; Zheng.Yulong@slm-solutions.com (Y.Z.); bernhard.roth@hot.uni-hannover.de (B.W.R.)
2 School of Engineering and the Built Environment, Edinburgh Napier University, Edinburgh EH10 5DT, UK; l.alwis@napier.ac.uk
3 Cluster of Excellence PhoenixD, (Photonics, Optics, and Engineering–Innovation Across Disciplines), 30167 Hannover, Germany
* Correspondence: Kort.Bremer@hot.uni-hannover.de; Tel.: +49-511-762-17905

Received: 18 November 2019; Accepted: 28 December 2019; Published: 2 January 2020

Abstract: An investigation on the feasibility of utilizing Mode Division Multiplexing (MDM) for simultaneous measurement of Surrounding Refractive Index (SRI) and temperature using a single sensor element based on an etched OM4 Graded Index Multi Mode Fiber (GI-MMF) with an integrated fiber Bragg Grating (BG), is presented. The proposed work is focused on the concept of principle mode groups (PMGs) generated by the OM4 GI-MMF whose response to SRI and temperature would be different and thus discrimination of the said two parameters can be achieved simultaneously via a single sensor element. Results indicate that the response of all PMGs to temperature to be equal, i.e., 11.4 pm/°C, while the response to SRI depends on each PMG. Thus, it is evident that temperature "de-coupled" SRI measurement can be achieved by deducing the temperature effects experienced by the sensor element. Sensitivity of the PMGs to applied SRI varied from 3.04 nm/RIU to of 0.22 nm/RIU from the highest to lowest PMG, respectively. The results verify that it is feasible to obtain dual measurement of SRI and temperature simultaneously using the same, i.e., single, sensing element.

Keywords: Mode Division Multiplexing (MDM); Few-Mode Fiber (FMF); principle mode groups (PMG); Bragg grating (BG); multi-mode fiber bragg grating; fiber optic sensor (FOS); multi-parameter sensing

1. Introduction

Despite the progress that had been already achieved on Mode Division Multiplexing (MDM) in the fiber optic communications sector, Fiber Optic Sensor (FOS) applications utilizing MDM is relatively unexplored. In this publication, the authors investigate the application of MDM that would allow the development of new sensor concepts. For instance, one FOS approach based on MDM could be Multi-Mode Fibers (MMF) incorporated with Bragg grating (BG) structures. Since every mode of the MMF has a different propagation constant, the inscription of a BG structure into the MMF would cause individual Bragg reflections for every mode. When combining a mode-selective excitation, such as grating assisted mode multiplexer [1,2] or Spatial Light Modulators (SLMs) [3], and a spectral interrogator, several BG structures could be wavelength multiplexed along the same optical fiber

and the additional mode-multiplexing would allow the discrimination between the different Bragg reflection of each BG structure. This, for instance, could allow the simultaneous measurement of the Surrounding Refractive Index (SRI) and temperature using only one BG structure, since different modes depends differently on the SRI.

Recent work by Yang et al. [4] demonstrated the capability of this concept by showing the simultaneous measurement of refractive index (RI) and temperature using an etched Few-Mode Fiber (FMF) with BG, termed FMFBG. The main mechanism of FMF follows that although BGs are insensitive to the SRI, when the cladding is sufficiently reduced, the evanescent field could interact with the surrounding media and the effective RI of the core would depend on the RI of the surrounding media. This has a direct impact on the resonance wavelength of the grating and thus the sensor is then sensitive to the SRI. Due to the different mode field distribution in the core and cladding region (and thus the effective refractive indices, n_{eff}, of the modes depend differently on the SRI), the Bragg wavelength of the *LP01* and *LP11* modes depend differently on applied SRI and temperature (the temperature sensitivity of the modes depends on thermally induced refractive index change and the thermal expansion coefficient [5]) and this feature allows simultaneous detection of these two parameters using only a single sensor element.

Compared to step-index MMF, Graded-Index (GI)-MMF have the unique property that some of the modes propagating inside the fiber have almost identical propagation constants, which causes the formation of principle mode groups (PMGs) [3]. This unique feature leads to the grouping of all modes propagating inside the GI-MMF into only a few PMGs, where each PMG is characterized by a single mode propagation constant. Consequently, when a BG is inscribed in a GI-MMF the corresponding transmission and reflection spectrum consists of only several dips and peaks, respectively [6]. In addition, lower order PMGs contain modes which are confined more in the center of the core whereas higher order PMGs contain modes that are confined at the core/cladding interface [7]. Therefore, when the cladding material of the GI-MMF is removed, higher order PMGs are thus more sensitive to RI changes of the surrounding compared to lower order PMGs [7] and thus this kind of fibers could form the basis for mode-multiplexed FOS concepts.

The work presented herein investigates whether GI-MMFs can be applied for mode-multiplexing in FOS applications and the simultaneous measurement of SRI and temperature. A schematic of the proposed fiber optic sensor-head is shown in Figure 1. By etching the fiber optic sensor-head the higher order PMG become sensitive to applied SRI variation and by inscribing the BG the higher order and lower order PMG can be discriminated at the optical detector by observing the individual Bragg reflection peaks. The advantage of this approach is that only a single sensor element would be required for the simultaneous detection of these two parameters and due to the relatively large core diameter of 50 µm (in case of the OM4 GI-MMF) the sensor elements remains stable even after etching compared to FMF (core etched down to 17 µm [8]) and SMF (core etched down to 3.4 µm [9]) approaches and thus more applicable to distributed FOSs in the field.

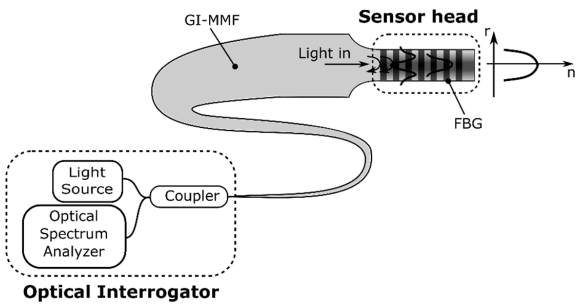

Figure 1. Schematic of the experimental setup for the etched OM4 Graded-Index Multi Mode Fiber (GI-MMF) with Bragg Grating (BG) for simultaneous measurement of Surrounding Refractive Index (SRI) and temperature using Principle Mode Group (PMG) multiplexing. The inset figure visualizes the general refractive index (n) distribution of a GI-MMF as a function of the fiber core radius (r).

2. Materials and Methods

2.1. Theoretical Background

When inscribing a BG into the core of GI-MMF the PMG formation causes that the Bragg condition is satisfied for modes of the same PMG or modes of neighboring PMGs [6]. The Bragg condition is given by:

$$\beta_1 - \beta_2 = 2\pi/\Lambda \tag{1}$$

where β_1 and β_2 are the propagation constants of the forward and backward propagating modes to be coupled and Λ is the grating period. In case of the coupling between modes of the same PMG, the propagation constants are equal $\beta = \beta_1 = -\beta_2 = 2{\cdot}\pi{\cdot}n_{eff}/\lambda$, where n_{eff} is the effective RI of the modes to be coupled, and from this the reflected Bragg wavelength for the coupled modes is calculated as [6]:

$$\lambda_B = 2n_{eff}\Lambda. \tag{2}$$

However, in case of the mode coupling between modes of neighboring PMGs the propagation constants are unequal with $\beta_1 = 2{\cdot}\pi{\cdot}n_{eff1}/\lambda$ and $\beta_2 = 2{\cdot}\pi{\cdot}n_{eff2}/\lambda$ and thus the corresponding reflected Bragg wavelength can be determined as follows [6]:

$$\lambda_B = \left(n_{eff1} + n_{eff2}\right)\Lambda \tag{3}$$

where n_{eff1} and n_{eff2} are the effective refractive indices of the coupled modes of the neighboring PMGs. From this it follows that the spectrum of a GI-MMF comprising a BG contains several peaks in reflection mode and several dips in transmission mode, where each peak and dip represents the mode coupling within the PMG of the same order and neighboring PMGs, respectively [6]. Consequently, lower order and higher order PMGs can be distinguished relatively easily by monitoring the reflection and/or transmission spectrum of the GI-MMF with BG, respectively, and observing the corresponding Bragg wavelength [6].

Furthermore, in Equations (2) and (3) the effective refractive indices depend on the field distribution of the modes to be coupled and thus this parameter can be sensitive to SRI, depending on whether a fraction of the electrical field of the mode is propagating inside the cladding or in the surrounding region.

2.2. Fabrication of GI-MMF FBGs

The GI-MMF BGs were fabricated on common OM4 GI-MMF from Corning©, using a KrF excimer laser (ATL Laser, UV inscription at 248 nm) and the phase mask technique. The OM4 GI-MMF was acrylate coated and had core and cladding diameters of 50 µm and 125 µm, respectively. To enable the inscription of BGs in the Germanium (Ge)-doped silica core, the OM4 GI-MMF was hydrogen loaded at a pressure of 200 bar for two weeks at room temperature (23 °C). Immediately after the hydrogen loading, the acrylate fiber coating was removed and 300 mm long fiber samples were exposed to the UV light from the KrF excimer laser with a repetition rate of 15 Hz, a pulse energy of 5 mJ and an inscription time of 2 min. The BG inscription length was 7 mm and the period of the applied phase mask was 1070 nm. The transmission spectrum of the inscribed BG was carefully monitored using a broadband light source (Thorlabs SLS201L/M) and an optical spectrum analyzer (Ando AQ6317B). An example of a transmission spectrum of a BG inscribed in the hydrogen loaded OM4 GI-MMF is shown in Figure 2. In total, 21 absorption dips of the fiber BG transmission spectrum were measured, where each absorption dip represents the Bragg reflection of an individual mode group and adjacent mode groups at the grating structure inside the GI-MMF [6] and the wavelength of the measured Bragg reflection peak decreases with increasing order of the mode groups, i.e., Bragg reflections peaks of the higher order mode groups are in the blue wavelength region.

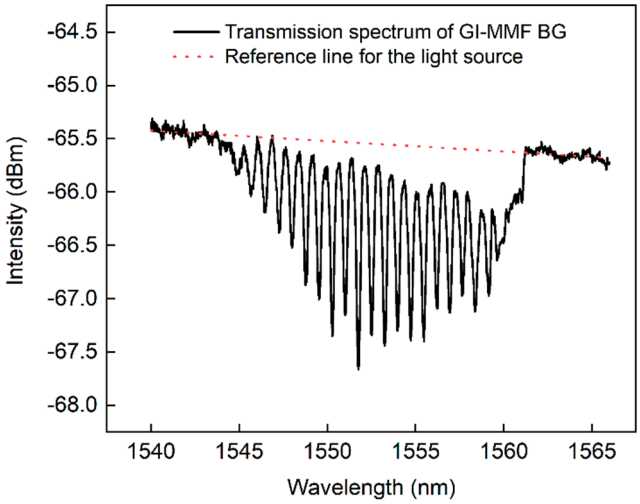

Figure 2. Measured transmission spectrum at a temperature of 20 °C of a BG written in OM4 GI-MMF using the phase mask technique. The red dashed line shows the reference intensity level of the applied light source.

Following the inscription of the BG, the cladding of the modified GI-MMF was removed over a length of 55 mm using hydrogen fluoride (HF) acid using the etching technique described elsewhere [2]. The final diameter of the etched fiber part was approximately 43 µm. In addition, after the etching process was complete, one end of the fiber containing the BG was spliced to the OM4 GI-MMF pigtail and the other end was cut close to the spatial position of the BG in order to obtain a single ended sensor probe, i.e., for RI and temperature measurement.

2.3. Experimental Set-Up

The experimental set-up shown in Figure 1 was developed to evaluate the response of the modified GI-MMF with BG to SRI and temperature variations. The sensor element was interrogated using a broadband light source (Opto-Link C-Band ASE) and an optical spectrum analyzer (Ando AQ6317B). In order to receive the reflection spectrum from the GI-MMF BG, a MMF 1 × 2 (all4fiber) coupler was applied. Since the output of the broadband light source is fiber coupled (SM, 9/125 µm core/cladding diameter), it was connected to a 2000 m OM4 GI-MMF coil where at the beginning of the coil the OM4 fiber was periodically bent with a bending radius of 5 mm and 30 turns in order to obtain equal excitation of the modes propagating in the GI-MMF (equilibrium mode distribution). A fiber length of 2000 m and a bend radius of 5 mm were chosen in order to prevent modal interferences as well as to obtain a relatively high fiber bending and enabling modal cross-talk without breaking the fiber.

In order to alter the SRI, different RI liquids (series A and AA) from Cargille Labs (n = 1.40, n = 1.42, n = 1.43, n = 1.45 and n = 1.47) and deionized water (n = 1.33) were applied. Cargille Labs specifies the refractive index of the liquids for an optical wavelength of 589.3 nm and a temperature of 25 °C. After each RI measurement, the sensor element was cleaned subsequently with acetone, ethanol and deionized water. The temperature response was measured by inserting the fiber sensor into a rectangular aluminum bar (100 × 20 × 20 mm^3) with an 8 mm diameter and 70 mm long borehole. The temperature of the aluminum bar was controlled using electrical resistors which were used as heating elements that were connected to a temperature controller (Quick-Cool QC-PC-CC-12). The reflection spectrum of each measurement was observed and saved using Labview and the measured sensor response was analyzed using Matlab. The wavelength shifts of the individual Bragg reflection peaks were obtained by determining the "center of mass" of each peak. Moreover, the Bragg reflection peaks in the wavelength region from 1549–1558 nm were analyzed and presented since reflection peaks in this wavelength range were consistent for all measurements.

3. Results

3.1. Response to Refractive Index Variations

The reflection spectrum of the etched GI-MMF BG at 20 °C for different SRI values is illustrated in Figure 3.

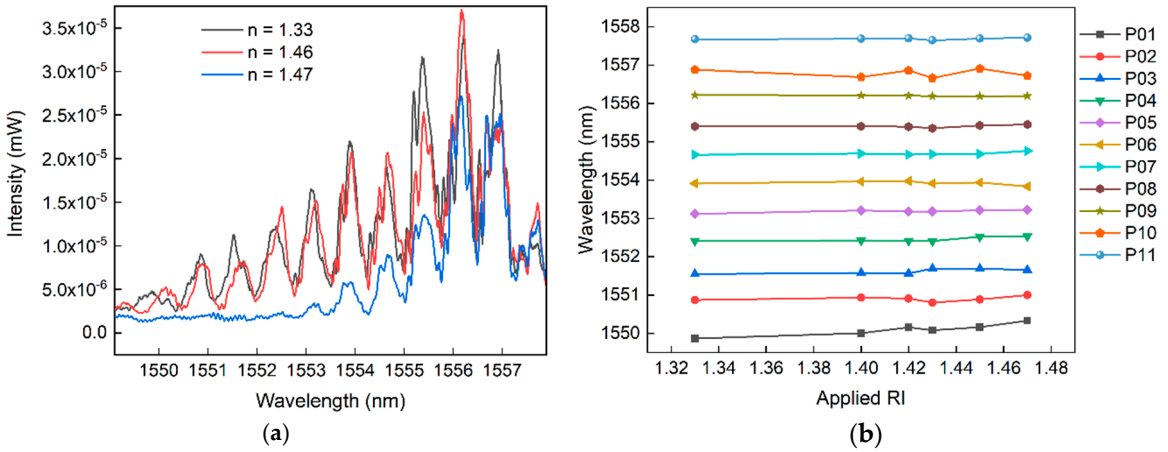

Figure 3. Reflection spectrum of etched GI-MMF with BG for different SRI values (**a**) and the response of the individual Bragg reflection peaks to different applied SRI values (**b**). *P01–P11* indicate the Bragg reflection peaks in the reflection spectrum from left to right, i.e., the Bragg reflection peak of the highest PMG is marked with *P01*, whereas the Bragg reflection peak of the lowest PMG is marked with *P11*.

Since the diameter of the GI-MMF containing the BG was only 43 µm after the etching procedure, the measured reflection spectrum illustrated in Figure 3a contains a lower number of reflection peaks in the left-hand side (blue wavelength range) compared to the measured transmission spectrum shown in Figure 2, i.e., no Bragg reflection peaks below 1549 nm were measured after etching the optical fiber. In addition, at an SRI of $n = 1.47$ the reflection amplitudes of the higher order PMGs decrease, as depicted in Figure 3a. This can only be explained by modes that are confined at the core/cladding interface, i.e., when the etched fiber sensor-head is immersed into a solution with a higher RI compared to the fiber core, these modes of the higher order PMGs are coupled out of the optical glass fiber which thus results in power loss. Therefore, only modes of higher order PMGs are able to interact with the environment and thus are capable to shift the Bragg reflection wavelength depending on the RI of the surrounding. Moreover, as depicted in Figure 3a the envelope of the measured reflection spectra of the sensor varies with different SRI and thus makes the exact determination of the Bragg reflection peak wavelength for each SRI value difficult (discussed in Section 4). In Figure 3b also the response of the fabricated sensor element to RI variations is illustrated. In total of 10 measurements were performed for each refractive index solution and only the obtained mean values are depicted in Figure 3b. The corresponding sensitivity of the individual Bragg reflection peaks are summarized in Table 1.

Table 1. Sensitivities of the different Bragg reflection peaks to applied SRI.

	P01	***P02***	***P03***	***P04***	***P05***	***P06***	***P07***	***P08***	***P09***	***P10***	***P11***
nm/RIU	3.04	0.47	0.98	0.81	0.71	−0.35	0.47	0.24	−0.21	−0.61	0.22
R^2	0.88	0.12	0.56	0.49	0.81	0.11	0.38	0.12	0.80	0.07	0.19

From the obtained response, it follows that for increasing order of the PMG, a trend toward higher sensitivity to SRI can be seen, which agrees well with the literature [7]. The value R^2 in Table 1 specifies the coefficient of linear regression of the sensitivity for each PMG. From the obtained R^2 values it

follows that for a decreasing PMG order, a trend towards negligible or no sensitivity to applied RI was measured. Moreover, the PMGs *P06*, *P09* and *P10* show a negative sensitivity to applied RI. However, this error in measurement is attributed to the optical interrogation system (see Section 4). In Figure 4 the relative wavelength shifts of the Bragg reflection peaks *P01* and *P11* for different SRI are shown for the 10 measurements performed for each refractive index solution. A standard deviation of 0.064 nm has been obtained for the refractive index measurements using the Bragg reflection peak *P01*.

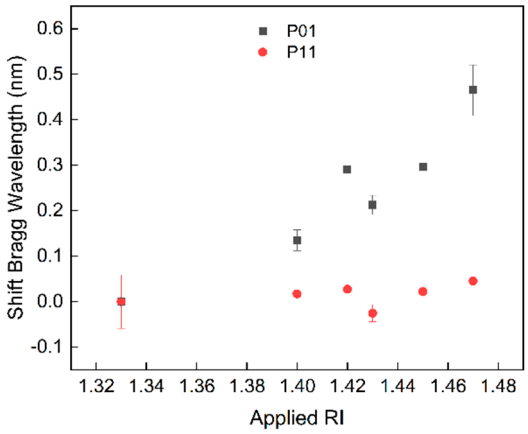

Figure 4. Bragg wavelength shift for the highest (*P01*) and lowest (*P11*) PMG for different SRI solutions.

3.2. Response to Temperature Variations

In Figure 5 as well as Table 2, the response of the individual Bragg reflection peaks to applied temperature is illustrated for a constant RI (air). Ten measurements were performed for every temperature step and the obtained mean values for the measured Bragg reflection peaks per temperature step are depicted in Figure 5.

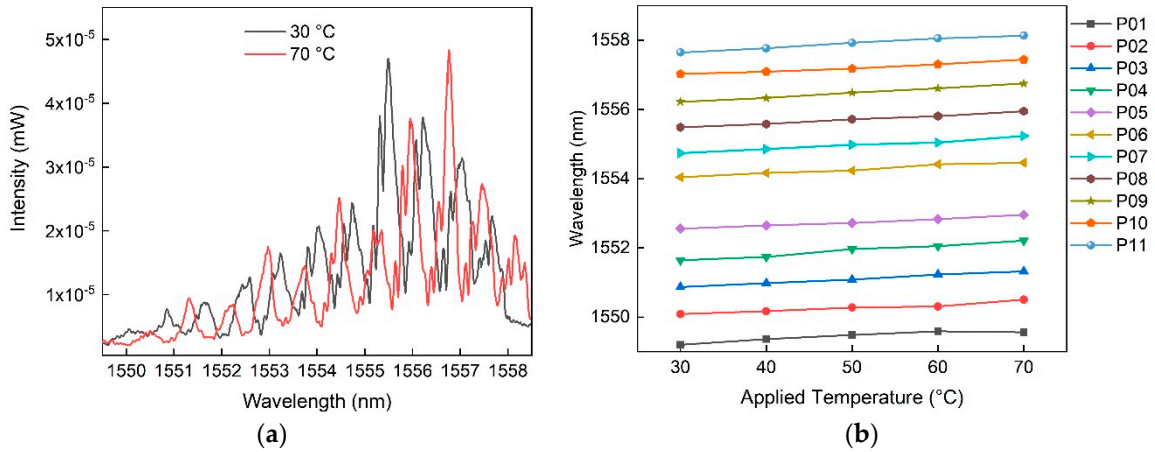

Figure 5. Reflection spectrum of etched GI-MMF with BG for the measurement of different surrounding temperatures (**a**) and the response of the individual Bragg reflection peaks to different applied temperature values (**b**) *P01–P11* indicate the Bragg reflection peaks in the reflection spectrum from the left to the right, i.e., the Bragg reflection peak of the highest PMG is marked with *P01*, whereas the Bragg reflection peak of the lowest PMG is marked with *P11*.

Table 2. Sensitivities of the different Bragg reflection peaks to applied temperature.

	P01	***P02***	***P03***	***P04***	***P05***	***P06***	***P07***	***P08***	***P09***	***P10***	***P11***
pm/°C	9.6	9.7	11.6	14.3	9.8	10.9	11.8	11.6	13.4	10.5	12.6
R^2	0.88	0.95	0.99	0.98	0.99	0.97	0.98	0.99	0.99	0.98	0.99

According to the results obtained, all individual Bragg reflection peaks show linear behavior (R^2 value $\geq$ 0.88) as well as an almost identical sensitivity to applied temperature (on average 11.4 pm/°C). This result is consistent with the literature (11.5 pm/°C) for GI-MMF [6]. Since all modes have almost the same thermo-optic coefficient all Bragg reflection peaks show almost identical temperature sensitivity [6]. A standard deviation of 0.014 nm has been obtained for the temperature measurements using the Bragg reflection peak *P11* (since *P11* exhibit negligible or no sensitivity to applied RI, it is more suitable for the determination of applied temperature), for instance.

4. Discussion

The obtained results verify that higher order PMGs are more sensitive to SRI variations compared to lower order PMGs. In addition, results obtained are consistent with reported results for GI-MMF [6] (in case of the response to temperature) and FMF [4] (in case of the response to SRI) in the literature. Consequently, it can be shown that by applying the single sensor element and PMG multiplexing, the simultaneous measurement of RI and temperature is feasible. However, the applied interrogation system which is based on equilibrium mode excitation and the applied Bragg wavelength peak detection ("center of mass" determination) is not sufficient to prove the simultaneous measurement of both parameters at the moment as the envelope of the measured Bragg reflection peaks of the etched GI-MMF with BG varies for different SRI values (see Figure 3a). The change of the envelope for every SRI value can be explained by the different sensitivities to SRI of the modes (the amount of the evanescent field spread in the surrounding varies depending on the mode) of each PMG and thus the corresponding Bragg wavelength change of each mode varies differently with different RI values. This causes a broadening of the individual Bragg reflection peaks. Another reason for the change of the envelope of the measured spectrum for different refractive indices might be the handling of the sensor element and immersion into the different RI solutions. Since the fiber was moved and held in another position for each RI solution, the power of the different modes might vary slightly (through change in the equilibrium mode distribution) and thus the envelope of the reflected FBG spectrum might fluctuate.

Since the ultimate goal of achieving a mode-multiplexed sensor system requires the excitation of individual modes, the interrogation system shown in Figure 1 is currently being modified by adding a SLM to the optical path. Therefore, in the next configuration, the new interrogation system will allow the individual excitation of certain modes of each PMG (modes that propagate mostly at the core/cladding interface or only within the core of the sensor element) and thus the uncertainty of the peak detection due to envelope changes will be eliminated. Compared to other BG based fiber optic RI sensors, which had reported, i.e., a sensitivity of 71.2 nm/RIU [10], the obtained RI sensitivity of the proposed sensor system is relatively low. Therefore, in future research different techniques to increase the RI sensitivity will also be explored, such as coating the fiber optic sensor with thin polymer overlays [11].

5. Conclusions

In this work a single sensor element based on an etched OM4 GI-MMF with integrated BG was proposed and investigated for simultaneous determination of applied temperature and SRI. Experimental results verify that different PMGs respond differently to applied SRI but equally to applied temperature. Therefore, by applying PMG multiplexing and a single sensor element consisting of an etched GI-MMF with BG, the simultaneous measurement of SRI and temperature is feasible. Experiments show that the sensitivity to SRI increases with increasing order of the PMG. Sensitivities of 3.04 nm/RIU and of 0.22 nm/RIU to applied SRI in the range from 1.33 and 1.47 for the highest and lowest PMG, respectively, were obtained. The temperature sensitivity of all PMGs was almost equal. The obtained standard deviation of the SRI and temperature measurement were 0.064 nm (for *P1*) and 0.014 nm (for *P11*). Further work is being carried out presently on a new interrogation system which would allow the excitation of individual modes of the etched GI-MMF. Thus, the interrogation system

will then compensate for the envelope fluctuations of the measured reflection spectrum which limits the detection of the wavelength shift of the Bragg reflection peaks due to applied SRI. Additionally, the enhancement of the sensitivity to SRI will be investigated by using thin polymer overlays [11] as well as whether the new sensor element can be applied for simultaneous measurement of humidity [12] and temperature or strain and temperature by using different sensor coatings. In future experiments, the temperature range of the proposed sensor element will also be investigated.

Author Contributions: Conceptualization: K.B.; software: K.B.; validation: K.B., L.S.M.A. and Y.Z.; investigation: K.B., Y.Z., L.S.M.A.; writing—original draft preparation: K.B. and L.S.M.A.; writing—review and editing: B.W.R.; supervision: B.W.R. All authors have read and agreed to the published version of the manuscript.

Funding: Bernhard Roth acknowledges funding from the Deutsche Forschungsgemeinschaft (DFG, German Research Foundation) under Germany's Excellence Strategy within the Cluster of Excellence PhoenixD (EXC 2122, Project ID 390833453).

Acknowledgments: The authors would like to acknowledge the work from Jörg Neumann, Michael Steinke and Sebastian Böhm from the Laser Zentrum Hannover for etching the GI-MMF.

Conflicts of Interest: The authors declare no conflict of interest.

References

1. Bremer, K.; Lochmann, S.; Roth, B. Grating assisted optical waveguide coupler to excite individual modes of a multi-mode waveguide. *Opt. Commun.* **2015**, *356*, 560–564. [CrossRef]
2. Schlangen, S.; Bremer, K.; Böhm, S.; Wellmann, F.; Steinke, M.; Neumann, J.; Roth, B.; Overmeyer, L. Grating assisted glass fiber coupler for mode selective co-directional coupling. *Opt. Lett.* **2019**, *44*, 2342–2345. [CrossRef] [PubMed]
3. Franz, B.; Bulow, H. Experimental Evaluation of Principal Mode Groups as High-Speed Transmission Channels in Spatial Multiplex Systems. *IEEE Photonics Technol. Lett.* **2012**, *24*, 1363–1365. [CrossRef]
4. Yang, H.Z.; Ali, M.M.; Islam, M.R.; Lim, K.; Gunawardena, D.S.; Ahmad, H. Cladless few mode fiber grating sensor for simultaneous refractive index and temperature measurement. *Sens. Actuators A* **2015**, *228*, 62–68. [CrossRef]
5. Kashyap, R. *Fiber Bragg Gratings*, 2nd ed.; Academic Press: New York, NY, USA, 2009.
6. Mizunami, T.; Djambova, T.V.; Niiho, T.; Gupta, S. Bragg gratings in multimode and few-mode optical fibers. *J. Lightwave Technol.* **2000**, *18*, 230–235. [CrossRef]
7. Kezmah, M.; Donlagic, D. Multimode all-fiber quasi-distributed refractometer sensor array and cross-talk mitigation. *Appl. Opt.* **2007**, *46*, 4081–4091. [CrossRef] [PubMed]
8. Fernandes, D.; Winter, R.; Da Silva, J.C.C.; Kamikawachi, R.C. Influence of temperature on the refractive index sensitivities of fiber Bragg gratings refractometers. *J. Microw. Optoelectron. Electromagn. Appl.* **2017**, *16*, 385–392. [CrossRef]
9. Chryssis, A.N.; Lee, S.M.; Lee, S.B.; Saini, S.S.; Dagenais, M. High sensitivity evanescent field fiber Bragg grating sensor. *IEEE Photonics Technol. Lett.* **2005**, *17*, 1253–1255. [CrossRef]
10. Wei, L.; Huang, Y.; Xu, Y.; Lee, R.K.; Yariv, A. Highly sensitive fiber Bragg grating refractive index sensors. *Appl. Phys. Lett.* **2005**, *86*, 151122. [CrossRef]
11. Alwis, L.; Bremer, K.; Sun, T.; Grattan, K.T.V. Analysis of the Characteristics of PVA-Coated LPG-Based Sensors to Coating Thickness and Changes in the External Refractive Index. *IEEE Sens. J.* **2013**, *13*, 1117–1124. [CrossRef]
12. Alwis, L.; Sun, T.; Grattan, K.T.V. Analysis of Polyimide-Coated Optical Fiber Long-Period Grating-Based Relative Humidity Sensor. *IEEE Sens. J.* **2012**, *13*, 767–771. [CrossRef]